International Journal on Magnetic Particle Imaging
Vol 11, No 1, Article ID 2508002, 7 Pages

Infinite Science Publishing

Research Article

Magnetic Staging in Sentinel Lymph Node Procedures: Insights from the LowMag Trial

Sadaf Salamzadeh[a] · Anke Christenhusz[b] · Anneriet E. Dassen[b] · Heleen.S van Nie[a] · Hermen Voerknecht[a] · Erik H.J.G. Krooshoop[a] · Bennie ten Haken[a] · Lejla Alic[a,*]

[a]Magnetic Detection & Imaging Group,Technical Medical Centre, University of Twente, The Netherlands
[b]Department of Surgery Medisch Spectrum Twente, Enschede, The Netherlands
*Corresponding author, email: lejlaresearch@gmail.com

Received 01 November 2024; Accepted 02 June 2025; Published online 26 August 2025

Abstract

Accurate identification of metastatic sentinel lymph nodes (SLNs) is essential for cancer prognosis and treatment planning. In the LowMag clinical trial, a magnetic sentinel lymph node biopsy (SLNB) procedure was implemented in patients with invasive breast cancer. This study evaluates the iron content and AC magnetic susceptibility of SLNs containing magnetic tracer to differentiate between metastatic and non-metastatic SLNs. Two magnetic detection devices, the superparamagnetic quantifier (SPaQ) and the differential magnetometer handheld (DMH) probe, were used to measure iron content and magnetic susceptibility of individual SLNs. Additionally, ex vivo low-field MRI and detailed histopathology were conducted. A total of 37 SLNs from 20 consecutive patients, including four metastatic SLNs, were analysed. Iron quantification by low-field MRI and histopathology correlated well with measurements from the DMH probe and SPaQ. A statistically significant difference in iron content was observed between metastatic SLNs (N = 4; DMH: 203.12 ± 87.67 µg , SPaQ: 131.28 ± 53.38 µg) and non-metastatic LNs (N = 33; DMH: 92.47 ± 89.8 µg, SPaQ: 42.45 ± 46.9 µg). Moreover, the combination of DiffMag counts with two features derived by SPaQ from the AC susceptibility (ACS) curve - Full Width at Half Maximum (FWHM) and peak value - achieved 66.7% sensitivity for detection metastatic SLNs, 93.3% specificity for non-metastasis detection, and overall accuracy of 90.9%. These numbers for the DMH probe were 75.0% sensitivity, 78.8% specificity, and 78.4% accuracy. These findings suggest that the DiffMag method offers more precise detection of non-metastatic SLNs compared to metastatic ones. Notably, in both DiffMag and ACS modes, the SPaQ device outperformed the DMH probe in terms of specificity and overall accuracy, likely due to its specialized design.

I. Introduction

Identifying metastatic sentinel lymph nodes (SLNs) is crucial for prognosis and treatment of cancer patients. Historically, the status of regional SLNs in breast cancer patients was assessed by axillary lymph node dissection (ALND), combined with hisopathological evaluation of all removed SLNs. However, this approach is associated with high morbidity and costs, especially considering that a significant proportion of patients are node-negative [1, 2]. To address this issue, a sentinel lymph node biopsy (SLNB) procedure was developed to identify and excise the first draining lymph node from the primary tumour, commonly referred to as SLN. This SLN serves as a key indicator of the regional lymphatic status, providing valuable insights into the potential cancer spread. The SLNB procedure not only allows for a less in-

vasive approach to staging cancer but also enhances the accuracy of cancer diagnosis and treatment planning [3].

The current global standard for SLNB relies on the use of a radioactive tracer, often combined with blue dye [1]. While effective, this technique presents logistical challenges related to the handling and management of radioisotopes. Moreover, the use of radioactive materials introduces additional challenges including limited availability and strict regulatory requirements under ionizing radiation protection directive, and concerns regarding radioactive decay [3]. The potential radiation exposure to both patients and healthcare professionals further adds to the complexity of the procedure.

A new approach utilizing superparamagnetic iron oxide nanoparticles (SPIONs) as tracer, in combination with a handheld magnetometer [4], allows for SLNB without the use of radiation which effectively addresses limitations of conventional approach [1]. However, currently available clinical magnetometer [1, 5] faces challenges related to signal interference from surgical metal instrument and the need for frequent calibration, which can contribute to prolonged surgical procedures [6]. Therefore, there is a clear need for a method capable of accurately distinguishing SPIONs from surrounding materials, including human tissues and surgical instruments , while also providing precise quantitative measurements of the SPIONs that migrate to SLNs from the primary tumour. Such quantification could ultimately serve as a valuable indicator for differentiating between metastatic and non-metastatic SLNs [7].

In our preliminary analysis [1], we assessed iron uptake of 20 lymph nodes using a CE-marked magnetometry probe (Sentimag®, Endomag, Cambridge, UK) alongside low-field MRI and SPaQ device operating in DiffMag mode. The findings revealed distinct patterns of magnetic tracer uptake across different regions of the lymph nodes. Notably, low-field MRI successfully differentiated fat, nodal tissue, and magnetic tracer based on signal intensity or texture, demonstrating its potential as a valuable tool for SLNs identification [1].

This study aims to quantify iron uptake in 37 SLNs following magnetic tracer injection and to assess the effectiveness of DMH probe and SPaQ device, and low-field MRI in distinguishing between metastatic and non-metastatic sentinel lymph nodes.

II. Methods and Materials

This study includes results from 20 consecutive patients with histologically confirmed invasive breast cancer visible on ultrasound imaging who participated in the LowMag clinical trial (TRN NL4713) during the period August 2021 to August 2023 [8]. As per LowMag protocol [1], each patient received a peritumoural injection of 1 mL (28 mg iron) of Magtrace® (Endomag, Cambridge, UK) within a few days prior to the surgery. Patient-specific details provided in supplementary Table I. This study analyzed the results from 37 SLNs, with four SLNs from four individual patients confirmed as metastatic through histopathological examination. On average, 1.85 SLNs were resected per patient, with the number ranging from 1 to 5 nodes per individual patient. The location and size of the primary tumours in the LowMag cohort are illustrated in Figure 1, while detailed patient and tumours information is provided in Supplementary Table I.

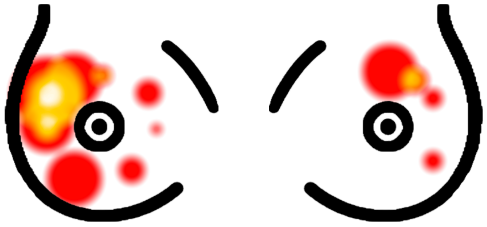

Figure 1: Distribution of primary tumour among the patients in LowMag study

Following surgery, all dissected SLNs were inked with three distinct colors using the Davidson Marking System® (Bradley Products, Inc.), as illustrated in Figure 2, to preserve orientation for both ex vivo data acquisition and subsequent histopathological analysis. The dissected SLNs were examined ex vivo using three different devices: a DiffMag handheld (DMH) prob [4, 9], a custom-built tabletop magnetometer device known as SPaQ [10], and a low-field tabletop MRI system [1]. The trapped iron in the SLNs was assessed using both DMH probe and SPaQ device, each operating in DiffMag mode [4, 6, 9].

As per LowMag protocol [1], the SLNs were transferred to pathology laboratory for histopathological examination directly after magnetic data acquisition. After fixation in buffered formalin, the three-coloured SLNs were lamellated at 250 μm along the black-inked side, and enclosed in a cassette for further histopathological processing. The embedded lamella was sectioned with the microtome at 2 μm distance and stained with H&E, Perls Prussian Blue (PPB), CK8/18 and CD68. H&E staining is specific for tissue morphology, provides information on the cell structure including nuclei (blue-purple) and cytoplasm (pink). Reduced cytoplasm volume is an indicator of cancerous cells [11]. Cytokeratin 8/18 (CK8/18) marker functions as a prognostic indicator in metastasis tissue and appears brown in histopathology [1, 12]. CD68 is the tumour associated macrophages marker with higher presence in non-metastasis SLNs [1, 13]. PPB stain is a marker to recognize iron in sentinel lymph nodes [1, 14]. The pathologist conducted comparative analysis across all four stains for a number of relevant regions of interest (ROIs). The focus was on

10.18416/ijmpi.2025.2508002

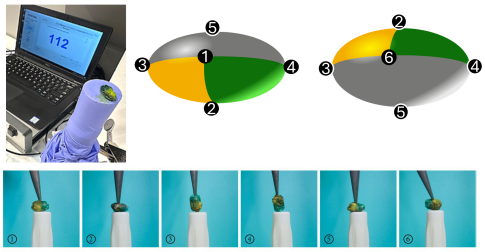

Figure 2: DMH probe assessment of iron content in SLNs across six different spots

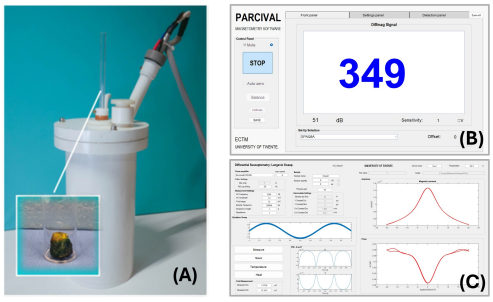

Figure 3: A) SPaQ tabletop magnetometer device assessing; B) DiffMag counts; C) AC susceptibility of lymph nodes

establishing correlations between macrophages, metastases and iron accumulation.

II.I. DMH prototype handheld probe

The DMH prototype includes a base unit, processing software, and a 2 cm diameter DMH probe featuring an excitation coil surrounded by two identical detection coils. The excitation coil generates a combined magnetic field sequence comprising a high-frequency AC component and offset fields, while the detection coils, positioned in series with reversed polarities, operate in a gradiometric configuration. This design passively cancels the excitation field, enabling accurate measurement of the SPIONs magnetization without being affected by the excitation field [4]. For the ex vivo SLNs analysis using the DMH probe, the frequency and amplitude of the AC excitation current were set at 2.5 kHz and 0.4 A, respectively. The offset excitation current amplitude was adjusted to 1 A with a 40% duty cycle. Under these settings, the applied magnetic field near the probe tip reaches approximately 1.8 mT.

During the experiment, each dissected SLN was placed on the probe's surface cover (Figure 2) in six distinct spots. DiffMag counts [15] were recorded for each orientation, with the highest count selected for further data analysis. This approach accounted for variations in lymph node positioning, ensuring that the maximum count provided the most reliable indication of the presence of the SPIONs, reducing underestimation due to probe-sample misalignment. The maximum and minimum readout counts for each SLN are provided in Supplementary Table I. DiffMag counts scale with the iron concentration. The iron uptake in each SLN was estimated according to the maximum reported count using a custom-designed lookup table (LUT) specifically tailored for Magtrace® concentrations relevant for the SLNB procedure [16].

II.II. SPaQ tabletop device

The Superparamagnetic quantifier is an in-house developed magnetometer [10] with detection and excitation coils that creates a uniform magnetic field with a glass sample holder positioned at the center of the homogeneous excitation field (Figure 3). It operates in two different modes: DiffMag and ACS.

SPaQ operating in the DiffMag mode [17], primarily generates a uniform magnetic field with an excitation sequence across the SLNs, similar to that of the DMH probe. This ensures consistent exposure throughout the entire sample. The uniformity of the magnetic field helps to minimize variability in the recorded DiffMag counts, regardless of the sample orientation within the holder. SPaQ's setting in DiffMag mode including amplitude of offset excitation current, frequency and amplitude of AC excitation current were set to 3 A, 2.5 kHz, and 0.5 A, respectively, with a duty cycle of 40% [18]. These settings generate 4.9 mT offset field and 0.81 mT AC field. The iron uptake in each SLN was estimated using a custom-designed lookup table (LUT) tailored to Magtrace® in SPaQ magnetic field [19].

SPaQ, operating in ACS mode [20], produces a uniform magnetic field across the SLNs. The excitation sequence takes place within a low-frequency field that lasts for one second, featuring a frequency of 1.5 Hz and an amplitude of 12 mT. This low-frequency excitation signal consists of a sinusoidal waveform with an amplitude of 1.2 mT and spans a frequency ranging $0.5-10$ kHz. In this study, the sinusoidal sequence frequency for ACS acquisition mode was set at 2.5 kHz. The dm/dH versus H curve was analyzed to extract parameters such as peak value and full width at half maximum (FWHM),where m represents the magnetic moment and H is the applied field. FWHM, which represents the spread of the point spread function, along with the peak value of ACS, yield valuable insights into the magnetic properties of iron uptake in the SLNs, including their dynamic magnetization [21, 22].

II.III. Low-field MRI

The resected SLNs were imaged using a low-field tabletop MRI system (Pure Devices GmbH, Rimpar, Germany), which features an enlarged bore size of 15 mm in diame-

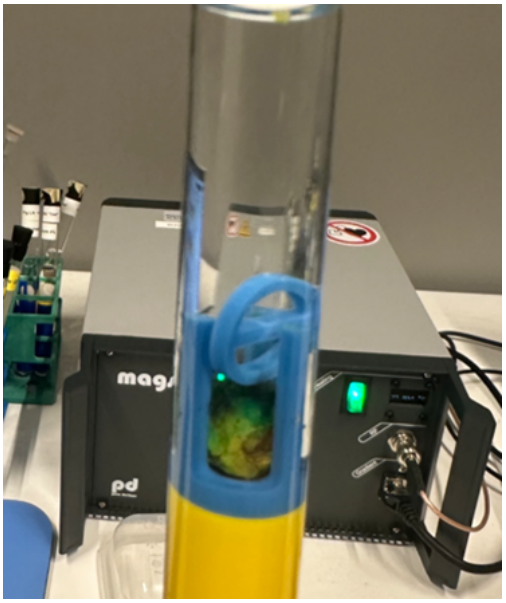

Figure 4: Tabletop MRI with modified bore size

ter and operates at a field strength of 0.5 T, shown in Figure 4. The imaging protocol involved acquiring 3D spin echo images with a field of view of $14 \times 14 \times 14$ mm and an isotropic resolution of 125 μm: Spin echo T1-weighted (T1W), T2-weighted (T2W), short tau inversion recovery (STIR), and T2 map [23]. Since formalin was consistent element in all MRI images, we utilized it to normalize the weighted images.

II.IV. Predicting metastases

Logistic regression was conducted to predict metastatic status by utilizing ACS features along with assessed iron levels. Given the clear imbalance in the dataset, where the metastatic class [N = 4] had significantly fewer observations than the non-metastatic class [N = 33], we assigned a higher weight to the minority class in the logistic regression. This approach helps to address the disparities in class sizes. Data processing including statistical analyses (two-sample t-test, $p = 0.05$), image registration, and generating visualizations of data was performed using MATLAB 2023a.

III. Results

III.I. Iron quantitation by DiffMag principle

Table 1 presents the magnetic sensing results of sentinel lymph nodes with and without metastasis, obtained using the DMH probe and the tabletop SPaQ device. The correlation in iron content measured by the two devices

Table 1: Average amount of iron captured in metastatic and non-metastatic sentinel lymph nodes, along with the associated ACS features. Statistically significant differences (p = 0.05%) are highlighted in bold.

Average ± std	Metastatic	Non metastatic
Fe - DMH (μg)	203.12 ± 87.67	**92.47 ± 89.8**
Fe - SPaQ (μg)	131.28 ± 53.38	**42.45 ± 46.9**
ACS - Peak value[$\times 10^{-10}$]	**9.21 ± 3.47**	**2.99 ± 3.46**
ACS -FWHM (mT)	4.09 ± 0.16	5.05 ± 2.46

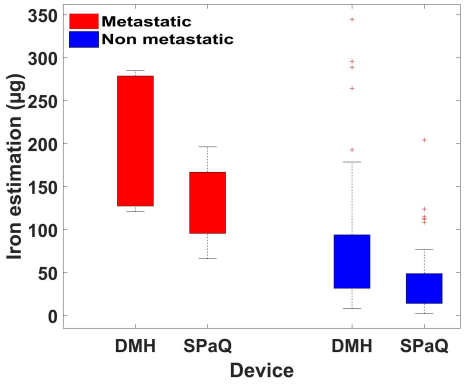

Figure 5: Iron uptake by sentinel lymph nodes with and without metastasis, using DMH probe and SPaQ

was 70% for metastatic SLNs and 84% for non-metastatic SLNs.

A paired two-tailed t-test was revealed significant differences between the devices in estimating iron uptake in non-metastasis SLNs ($p < 0.05$), however, not in metastasis SLNs ($p > 0.05$). Notably, the highest iron uptake was observed in a metastatic sentinel lymph node, averaging 285 μg of iron, which represents approximately 1% of the total injection dose.

As illustrates in Figure 5, both devices detected significantly elevated iron levels metastatic SLNs compared to non-metastatic sentinel lymph nodes.

The DMH readout counts for four metastatic SLNs, measured at various spots as outlined in Figure 2, are presented in Figure 6.

III.II. AC susceptibility of SLNs

Figure 7 presents the ACS signal for both metastatic and non-metastatic sentinel lymph nodes as a function of the applied magnetic field, measured using the SPaQ device in ACS mode. Table 1 presents the peak and FWHM for metastatic and non-metastatic SLNs separately [22].

Consistent with the DiffMag detection method, the average peak value of the ACS signal (Table 1) is notably higher in metastatic SLNs compared to non-metastatic

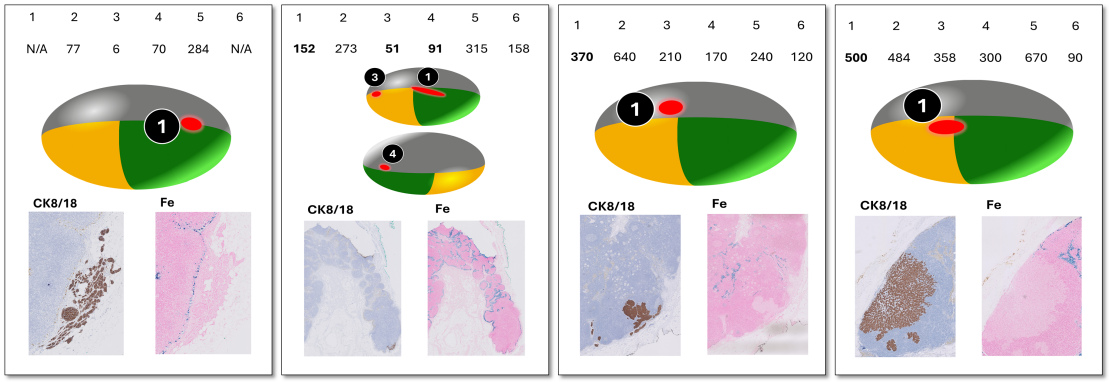

Figure 6: DMH probe assessment of iron uptake in four metastatic SLNs across six spots. Bold values indicate DiffMag counts in metastatic regions. CK8/18 and Fe-stained pathology images (lower panel) show reduced iron uptake in CK8/18-positive metastatic tissue.

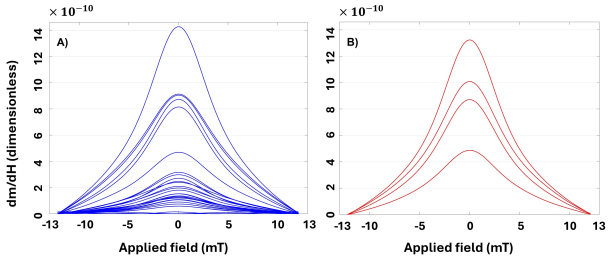

Figure 7: Changes in magnetization of sentinel lymph node containing iron A) non-metastasis, B) metastasis, within SPaQ device in ACS mode. Data for 4 non-metastatic SLNs in ACS measurements are unavailable.

ones, with an independent two tailed t-test confirming a significant difference ($p < 0.05$).

However, no significant differences were found in the FWHM values. MRI and histopathology images indicate that iron primarily accumulates in the sinusoidal regions of the sentinel lymph nodes, while the central areas remain largely free of iron. In both metastatic and non-metastatic SLNs, iron particles are densely packed within these regions, leading to relatively large FWHM. As a result, the spacial distributions of iron is similar for both metastatic and non-metastatic SLNs, leading to similar FWHM.

III.III. Assessment of SLN metastatic status

The accuracy of logistic regression for individual parameters listed in Table 1 was 78.4% for iron amount measured the DMH probe and 91.9% for those measures by the SPaQ device in DiffMag mode. For the ACS features, the peak value and FWHM yielded accuracies of 78.8% and 45.5%, respectively. When combining features, ACS features supplemented with DMH-measured iron content achieved an accuracy of 84.8% , while those combined with SPaQ-measure iron content reached 90.9%.

III.IV. Low field ttMRI

Figure 8 illustrates central-slice MRI alongside corresponding the pathology images for metastatic SLN (upper panel) and non-metastatic SLN (lower panel). These confirm the iron estimation by the DiffMag handheld probe and the SPaQ. The metastatic SLN, with a high estimated iron uptake (285 µg), appearing darker on the T2-weighted image, while the non-metastatic SLN, with lower iron content (39 µg), appearing brighter on the T2-weighted image.

Regardless of metastatic status, a fatty region is observed in both, showing no iron deposits or notable variation in formalin-normalized MRI. In metastatic lymph nodes, iron deposits are primarily located within the sinusoids LN regions, with minimal spread into the surrounding fat or metastatic tissue. Figure 6 provides detailed pathology images stained for CK8/18 and iron markers, highlighting zoomed-in metastatic regions from four individual metastatic SLNs - focusing specifically on areas containing metastatic tissue for clarity.

IV. Discussion

Breast cancer remains a major global healthcare challenge, and current imaging technique are unable to reliably stage SLNs for metastasis. As result, SLNB remains the standard for SLNs staging. In this ex vivo study, SLNs from female breast cancer patients were examined using two magnetometer devices and a tabletop MRI system. Both magnetometer devices successfully identified and quantified iron uptake, with amount of iron generally correlating with iron uptake patterns observed in pathology images. The DMH probe consistently reported higher

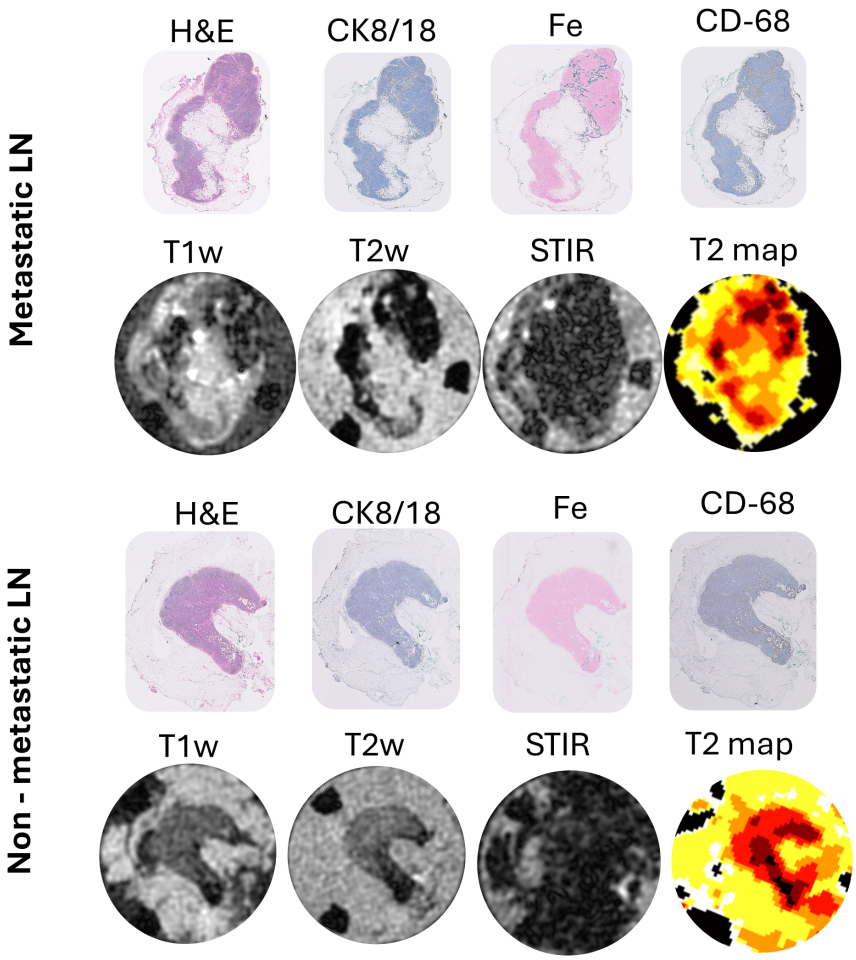

Figure 8: MRI and corresponding pathology images for a metastatic (upper panel) and non-metastatic (lower panel) sentinel lymph node. The MR images are windowed to increase visibility.

iron levels than the SPaQ device, which can be attributed to differences in device design. In the SPaQ system, the sample is positioned at the center of the applied magnetic field, resulting in an averaging effect of the magnetic moments. In contrast, the DMH probe aligns with a single direction of the magnetic field, allowing it to detect maximum changes in the magnetic moment.

The SPaQ device, operating in ACS-mode, showed the enhanced response in metastatic SLNs - likely due to differences in iron uptake or tumour-altered microenvironment. ACS signal characteristic may serve a potential surrogate biomarker for metastatic involvement. Specifically, analysis of ACS peak value and FWHM across SLNs revealed that combing these parameters may enable predictive classification of metastatic involvement. Comparison of the DMH probe and SPaQ device indicated that while both methods offer promise in enhancing diagnostic accuracy, SPaQ demonstrated higher diagnostic accuracy and specificity, making it a potentially more effective tool for clinical decision-making.

Tabletop MRI at $0.5T$ effectively differentiate between fat, nodal tissue, and magnetic tracer based on either signal intensity or texture, demonstrating its potential for compact intraoperative SLNs imaging.

V. Conclusion

This study revealed that less than 1% of the total injected iron accumulates in the SLNs. Despite this small fraction, both the DMH probe and the SPaQ tabletop device demonstrate potential for evaluating SLNs and identifying metastasis using SPIONs.

These findings underscore the importance of selecting the appropriate method for SPIONs quantification, as it can greatly influence the accuracy of cancer staging and diagnosis. Notably, even minimal amounts of retained

10.18416/ijmpi.2025.2508002

iron may offer valuable information about metastatic involvement.

Further research is warranted to better understand the underlying mechanisms behind these observations and to refine the clinical application of these magnetic sensing devices. This could enhance diagnostic precision and inform more effective treatment strategies for breast cancer and other cancers.

Author's statement

Conflict of interest: Authors state no conflict of interest.
Informed consent: Informed consent has been obtained from all individuals included in this study.
Ethical approval: The research related to human use complies with all the relevant national regulations, institutional policies and was performed in accordance with the tenets of the Helsinki Declaration, and has been approved by the authors' institutional review board or equivalent committee.

References

[1] A. Christenhusz, A. E. Dassen, M. C. van der Schaaf, S. Salamzadeh, M. Brinkhuis, B. ten Haken, and L. Alic. Magnetic procedure for sentinel lymph node detection and evaluation of metastases: Design and rationale of the lowmag trial. *BMC Methods*, 1(1):6, 2024, doi:10.1186/s44330-024-00006-3.

[2] E. R. Nieuwenhuis, B. Kolenaar, A. J. van Bemmel, J. J. Hof, J. van Baarlen, A. Christenhusz, J. J. Pouw, B. ten Haken, L. Alic, and R. de Bree. A complete magnetic sentinel lymph node biopsy procedure in oral cancer patients: A pilot study. *Oral Oncology*, 121:105464, 2021, doi:10.1016/j.oraloncology.2021.105464.

[3] S. Subramonian, S. Chopra, and R. Vidya. New alternative techniques for sentinel lymph node biopsy. *Medicina*, 2023, doi:10.3390/medicina59122077.

[4] S. Waanders, M. Visscher, R. R. Wildeboer, T. O. B. Oderkerk, H. J. Krooshoop, and B. ten Haken. A handheld spio-based sentinel lymph node mapping device using differential magnetometry. *Physics in Medicine & Biology*, 61(22):8120, 2016, doi:10.1088/0031-9155/61/22/8120.

[5] Endomag, Sentimag® - advanced surgical guidance. URL: https://www.endomag.com/en/products/sentimag/.

[6] E. R. Nieuwenhuis, N. Mir, M. M. Horstman-van de Loosdrecht, A. P. W. Meeuwis, M. G. J. de Bakker, T. W. J. Scheenen, and L. Alic. Performance of a nonlinear magnetic handheld probe for intraoperative sentinel lymph node detection: A phantom study. *Annals of Surgical Oncology*, 30(13):8735–8742, 2023, doi:10.1245/s10434-023-14166-z.

[7] Y. Yan, Y. Liu, T. Li, Q. Liang, A. Thakur, K. Zhang, W. Liu, Z. Xu, and Y. Xu. Functional roles of magnetic nanoparticles for the identification of metastatic lymph nodes in cancer patients. *Journal of Nanobiotechnology*, 2023, doi:10.1186/s12951-023-02100-0.

[8] C. C. M. O. (CCMO), A complete magnetic radiation free procedure for sentinel lymph node localization. URL: https://onderzoekmetmensen.nl/nl/trial/28812.

[9] M. Visscher, S. Waanders, H. J. Krooshoop, and B. ten Haken. Selective detection of magnetic nanoparticles in biomedical applications using differential magnetometry. *Journal of Magnetism and Magnetic Materials*, 365:31–39, 2014, doi:10.1016/j.jmmm.2014.04.044.

[10] M. Horstman - van de Loosdrecht, S. Draack, S. Waanders, J. Schlief, H. J. Krooshoop, T. Viereck, F. Ludwig, and B. ten Haken. A novel characterization technique for superparamagnetic iron oxide nanoparticles: The superparamagnetic quantifier, compared with magnetic particle spectroscopy. *Review of Scientific Instruments*, 90:024101, 2019, doi:10.1063/1.5039150.

[11] A. H. Fischer, K. A. Jacobson, J. Rose, and R. Zeller. Hematoxylin and eosin staining of tissue and cell sections. *CSH Protoc*, 2008, doi:10.1101/pdb.prot4986.

[12] M.-M. Shao, S. K. Chan, A. M. C. Yu, C. C. F. Lam, J. Y. S. Tsang, P. C. W. Lui, B. K. B. Law, P.-H. Tan, and G. M. Tse. Keratin expression in breast cancers. *Virchows Arch*, 2012, doi:10.1007/s00428-012-1289-9.

[13] J. Yang, X. Li, X. Liu, and Y. Liu. The role of tumor-associated macrophages in breast carcinoma invasion and metastasis. *Int J Clin Exp Pathol*, 2015.

[14] V. Bitonto, F. Garello, A. Scherberich, and M. Filippi, Prussian blue staining to visualize iron oxide nanoparticles, in *Histochemistry of Single Molecules: Methods and Protocols*, C. Pellicciari, M. Biggiogera, and M. Malatesta, Eds. Springer US, 2023. doi:10.1007/978-1-0716-2675-7_26.

[15] S. Salamzadeha, H. J. Krooshoop, B. ten Haken, and L. Alic. Diffmag handheld probe for perioperative lymph node harvesting. *International Journal on Magnetic Particle Imaging*, 9(1 Suppl. 1), 2023, doi:10.18416/IJMPI.2023.2303052.

[16] S. Salamzadeh and L. Alic, Look-up table for assessment of iron content in magtrace® samples based on sentimag®, 4TU.ResearchData, 2023.

[17] S. Waanders, M. Visscher, T. Oderkerk, H. J. Krooshoop, and B. ten Haken, Method and apparatus for measuring an amount of superparamagnetic material in an object, Patent, EP 12194029.0, 2012.

[18] L. Molenaar, M. M. H. van de Loosdrecht, L. Alic, J. van Baarlen, J. J. H. J. Meijerink, B. t. Haken, I. A. M. J. Broeders, and D. J. Lips. Quantification of magnetic nanoparticles in ex vivo colorectal lymph nodes. *Nano LIFE*, 12(03), 2022, Financial transaction number: 2500007318. doi:10.1142/S1793984422500064.

[19] L. Molenaar, Look-up table based on spaq measurements to quantify amount of iron in small samples, 4TU.Centre for Research Data, 2021. doi:10.4121/15034902.

[20] P. Kreissl, C. Holm, and R. Weeber. Frequency-dependent magnetic susceptibility of magnetic nanoparticles in a polymer solution: A simulation study. *Soft Matter*, 17:174–183, 1 2021, doi:10.1039/D0SM01554G.

[21] F. Mohn, K. Scheffler, J. Ackers, A. Weimer, F. Wegner, F. Thieben, M. Ahlborg, P. Vogel, M. Graeser, and T. Knopp. Characterization of the clinically approved mri tracer resotran for magnetic particle imaging in a comparison study. *Physics in Medicine & Biology*, 69(13):135014, 2024, doi:10.1088/1361-6560/ad5828.

[22] M. M. Horstman-van de Loosdrecht, T. Kahmann, F. Ludwig, and L. Alic. Tuning excitation field frequency for magnetic particle sensing using superparamagnetic quantifier. *Journal of Biomedical Nanotechnology*, 18(8):1994–2000, 2022, doi:10.1166/jbn.2022.3406.

[23] A. Christenhusz, F. F. J. Simonis, B. ten Haken, J. C. A. te Wildt, S. Salamzadeh, A. E. Dassen, and L. Alic, Ex vivo lymph node staging by a portable low-field mri scanner, in *Proceedings of the Joint Annual Meeting ISMRM–ISMRT*, Toronto, Canada, 2023.

